Zhuravlev A.V.[1], Vevel Y.A.[2]
All-Russia Petroleum Research Exploration Institute (VNIGRI), Saint Petersburg, Russia, [1]micropalaeontology@gmail.com, [2]Yadviga_Vevel@mail.ru

POSSIBILITIES OF COMPUTED MICROTOMOGRAPHY APPLICATION IN MICROPALAEONTOLOGICAL AND LITHOLOGICAL STUDIES

Possibilities of the computed X-ray and optic tomography in the micropalaeontological and lithological studies are considered. X-ray microtomography allows determining phosphate microfossils (conodonts) avoiding special sample preparation; evaluate the total porosity and concentration of sulfides. The optic microtomography promises results in histological study of conodont elements.

Key words: *tomography, micropalaeontology, conodonts, foraminifers, lithology, carbonates, silicites.*

Computed microtomography becomes the widely used method in different branches of the palaeontology and lithology last years [Withjack, 1988; Wellington, Vinegar, 1987; Peters, Afzal, 1992; Johns et al., 1993; Ketcham and Carlson, 2001; Arns et al., 2005; Tafforeau et al., 2006; Błażejowski et al., 2011; Zalewska, Kaczmarczyk, 2011]. This study is aimed to evaluation of the efficiency of tomographic methods in the micropalaeontological and lithological researches.

X-ray microtomography

Microfossils and lithological sample were scanned with an isotropic voxel resolution of 14-6.6 mkm at the Skyscan 1174 compact micro-CT (50 KV, 800 uA) of the Mining Institute at St.Petersburg. 3-dimensional reconstructions and tomogram processing were made using NRecon, DataViewer, CTvox (SkyScan), Voxler (Golden Software Inc.), and VolView 3 (Kitware Inc.) software.

Micropalaeontological objects

Conodont elements and foraminifera tests were investigated with the micro-CT equipment. The Pa elements of *Mehlina fitzroyi* (Druce), *Polygnathus lanei* Kuzmin (Middle Frasnian of the Main Devonian Field, East European Platform); *Polygnathus parapetus* Druce (Lower Tournaisian of the Pecjora Swell, Kamenka River section); *Polygnathus experplexus* Sandberg et Ziegler (Famennian of the Timan-Pechora Basin, Talota River section); *Siphonodella quadruplicata* (Branson et Mehl), *Siphonodella sandbergi belkai* Dzik, and *Siphonodella lobata* (Branson et Mehl) (Tournaisian of the Polar Urals, Kozhym River section); and S elements of Polygnathidae (Frasnian of the Main Devonian Field, East European Platform) represent studied conodont collection. Additionally conodont elements were found in the clayey silicite samples (Upper Tournaisian of the Polar Urals, Kozhym River section), and in the clayey limestone samples (Upper Frasnian of the Kosyu Depression, Timan-Pechora Basin).

Difference of physical properties of the hard tissues of conodont elements promises possibility to distinguish them in the X-ray images. However, low absorption contrast makes it impossible to recognize all the tissue types. Only two groups of tissues can be distinguished. The first one comprises “white matter”, lamellar, and interlamellar tissues. Paralamellar and, in some cases, lamellar tissues compose the second group. This group can be distinguished by higher X-ray absorption. The tissue spatial distribution can be used for conodont taxonomy [Zhuravlev, 2002]. CT-images allow us to improve histological models of the conodont elements studied (Figure 1).

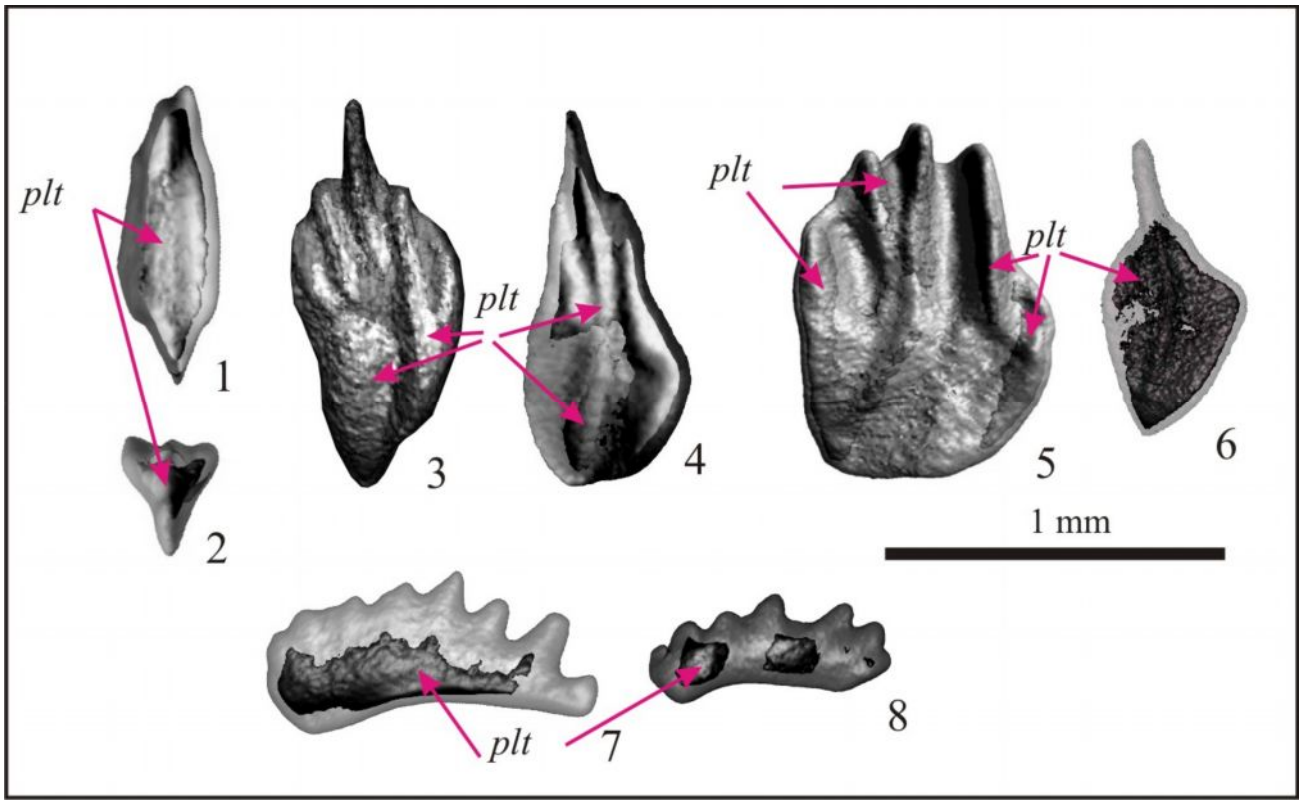

Figure 1. 3D histological models of the conodont elements based on the X-ray microtomograms
(visualization with Voxler software)

1, 2. - Polygnathus lanei Kuzmin, Pa element, sample 5102a-1; Main Devonian Field, Ilmen Lake; Upper Devonian, Frasnian, Polygnathus ilmenensis conodont zone.
3. - Siphonodella sandbergi belkai Dzik, Pa element, sample Tn-19e; Polar Urals, Konstantinov Creek; Lower Carboniferous, Tournaisian, Siphonodella quadruplicata Zone.
4. - Siphonodella quadruplicata (Branson et Mehl), Pa element, sample Tn-19e; Polar Urals, Konstantinov Creek; Lower Carboniferous, Tournaisian, Siphonodella quadruplicata Zone.
5. - Polygnathus experplexus Sandberg et Ziegler, Pa element, sample 0806-53/2k; Timan-Pechora Basin, Talota River; Upper Devonian, Famennian, Palmatolepis marginifera Zone.
6. - Siphonodella lobata (Branson et Mehl), Pa element, sample Tn-19e; Polar Urals, Konstantinov Creek; Lower Carboniferous, Tournaisian, Siphonodella quadruplicata Zone.
7. - Mehlina fitzroyi (Druce), Pa element, sample 5102a-1; Main Devonian Field, Ilmen Lake; Upper Devonian, Frasnian, Polygnathus ilmenensis conodont zone.
8. – Sc element of Polygnathidae, sample 5102a-1; Main Devonian Field, Ilmen Lake; Upper Devonian, Frasnian, Polygnathus ilmenensis conodont zone.
plt – paralamellar tissue.

High X-ray absorption of the conodont element matter (more than 20000 HU) makes conodonts distinguishable in the X-ray tomograms of the pieces of rocks. The tomogram images are suitable for taxonomic diagnostic of the elements (Figure 2). Thus it is possible to use CT for conodont study avoiding expansive sample preparation.

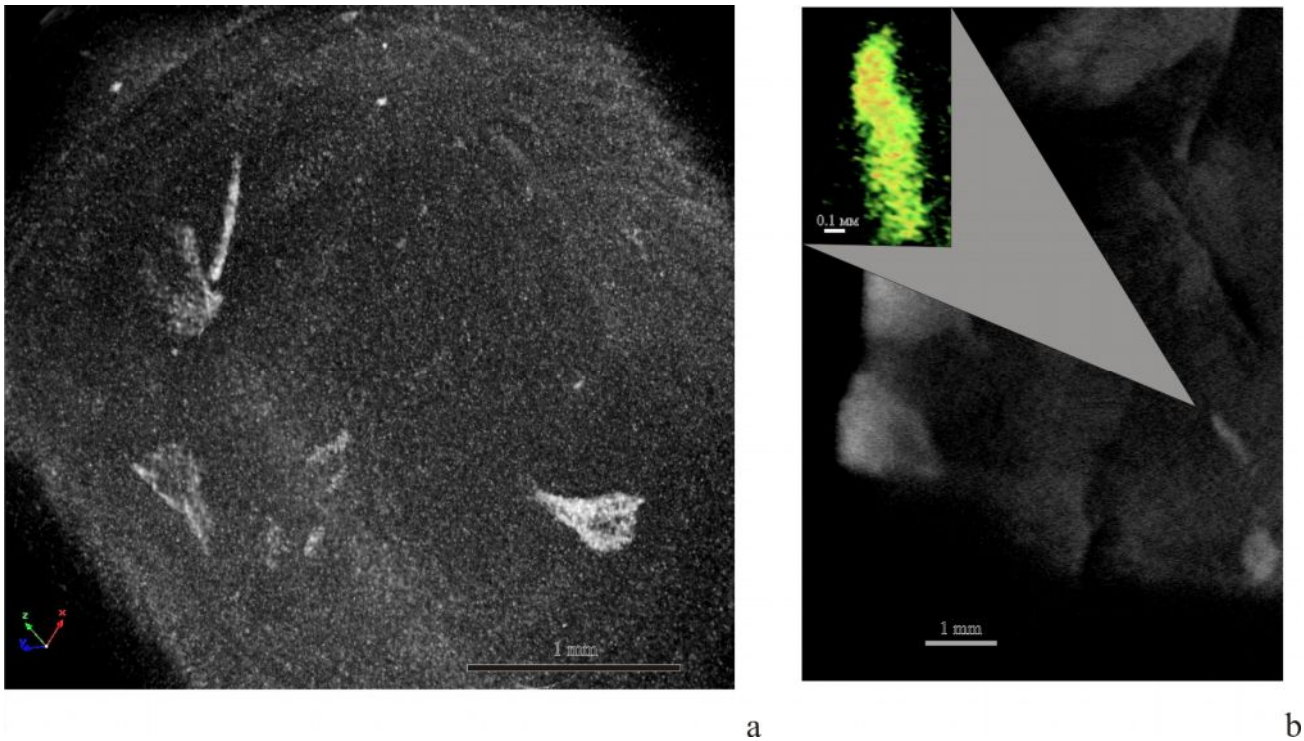

Figure 2. X-ray microtomograms of the rock pieces containing conodont elements

a – silicite (radiolarite) containing Pa elements of Siphonodella, sample Tn-23; Polar Urals, Konstantinov Creek; Lower Carboniferous, Tournaisian, Siphonodella quadruplicata Zone. Visualization with CTVox software.

b – clayey limestone containing Pa element of Polygnathus, sample HM-1-18; Timan-Pechora Basin, western part of the Kosyu Depression, borehole 1-Kharutamylk, depth 3367 m, Upper Devonian, Frasnian. Visualization with VolView 3 software.

The test of the Visean endothyrid foraminifera (East European Platform, Msta River section) of good preservation were studied with the micro-CT. The test matter demonstrates low X-ray absorption contrast that makes it difficult distinguishing morphological details (Figure 3). The CT-images allow us to recognise septa morphology, chamber shape in the last whorl, and measuring of the inner whorl diameter (Figure 3).

Lithological objects

Pieces of different types of the sedimentary rocks were selected for the X-ray CT study (Table 1). Total porosity, form and distribution of the pores, and sulfides content were reconstructed using the tomograms (Figure 4). The pores are distinguished in tomograms by low X-ray absorption (5000 HU in average) that differs from the X-ray absorption of the carbonates (6000-20000 HU). Sulfides, in contrast, are characterized by high X-ray absorption – more than 50000 HU (Figure 5).

Microstructures of clayey carbonates are distinguishable in X-ray tomograms due to prominent difference of the X-ray absorption of clay and calcite (Figure 5).

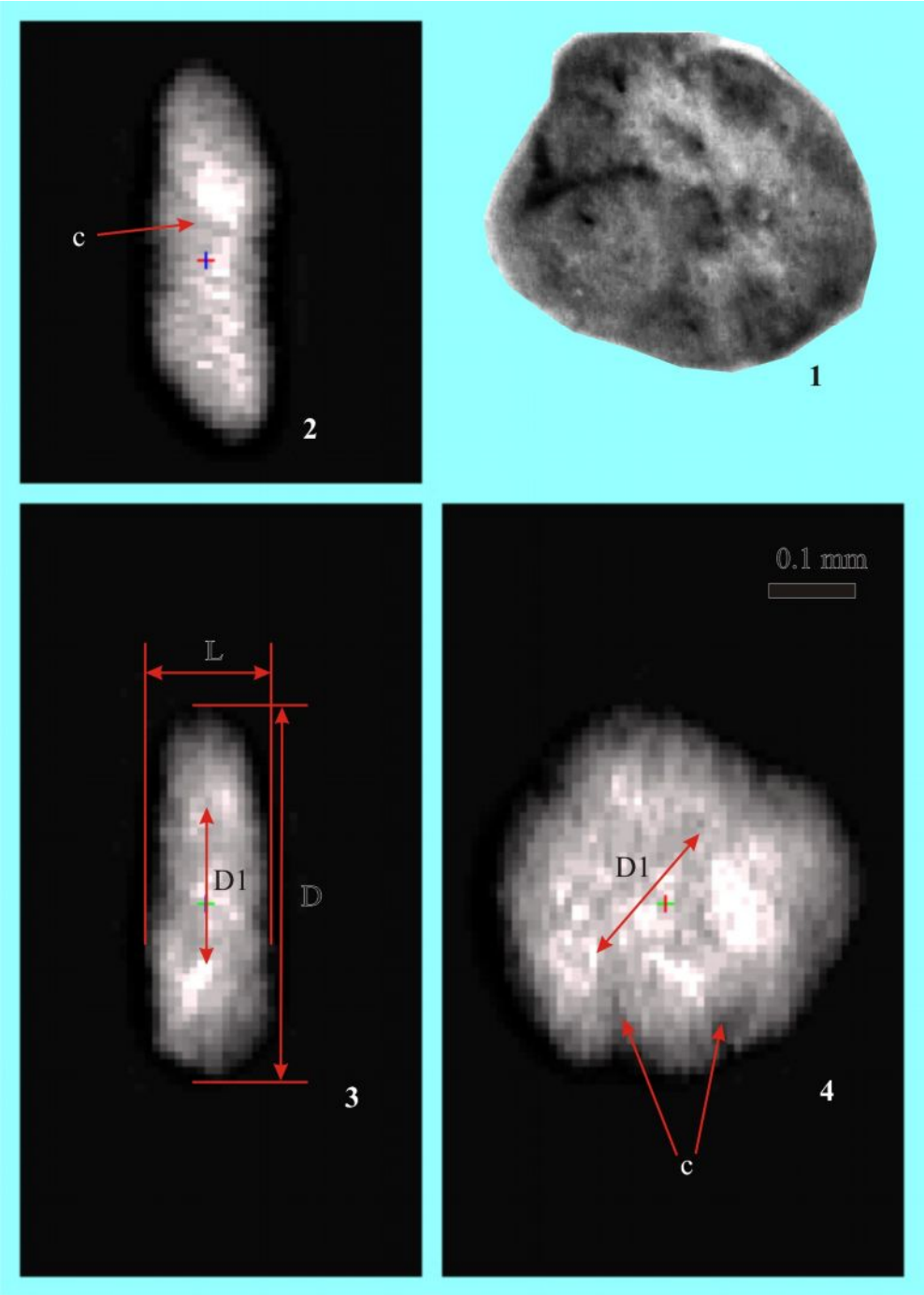

Figure 3. X-ray microtomogram of the endothyrid foraminifera test, sample S-1-3/05; NW of East European Platform, Msta River, Lower Carboniferous, Visean

1. – General view of the test.
2, 3. – Axial section.
4. – Median section.
D – diameter of the last whorl; D1 – diameter of the inner whorl; L – test height; C – septa.
Visualization with DataViewer software.

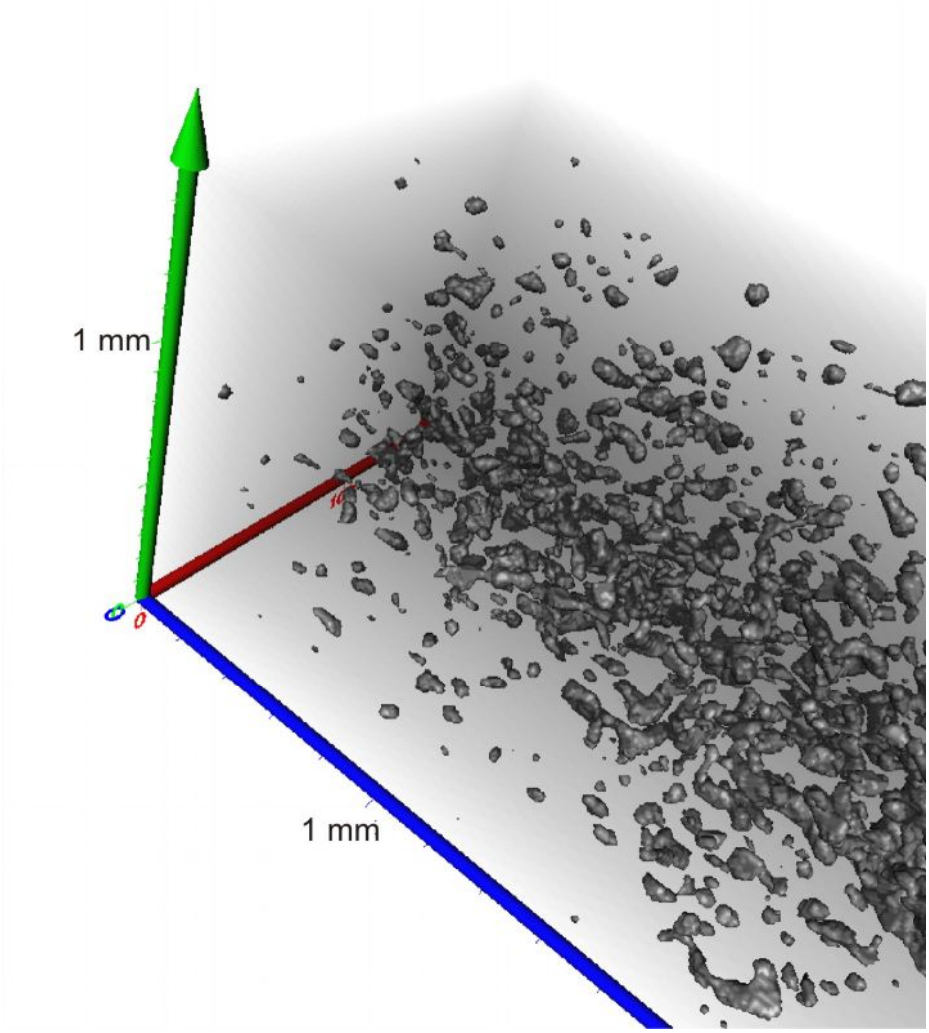

Figure 4. Pore distribution in the fine-grained limestone, sample 0806-208/1; north of the Timan-Pechora Basin, Talota River; Lower Carboniferous, Serpukhovian
Visualization with Voxler software.

X-ray micro CT allows measuring of the real grain sizes of the detritic limestones. The measurements were made with Voxler and DataViewer software. Tomogram preparation for the texture analysis includes high-frequency filtration and contrast enhancement.

Optic tomography

Microfossils and lithological sample were scanned with an isotropic voxel resolution of 16-1.9 mkm at the experimental optical microtomographs in visible light. 3D reconstructions and tomogram processing were made using NRecon, DataViewer, CTvox (Skyscan), and VolView 3 (Kitware Inc.) software.

Micropalaeontological objects

The optic tomograms of a number of conodont elements were made up. The studied conodont collection comprises S elements of Polygnathidae; Pa element of *Mehlina fitzroyi* (Druce) and juvenile Pa element of *Siphonodella quadruplicata* (Branson et Mehl) (Figure 6).

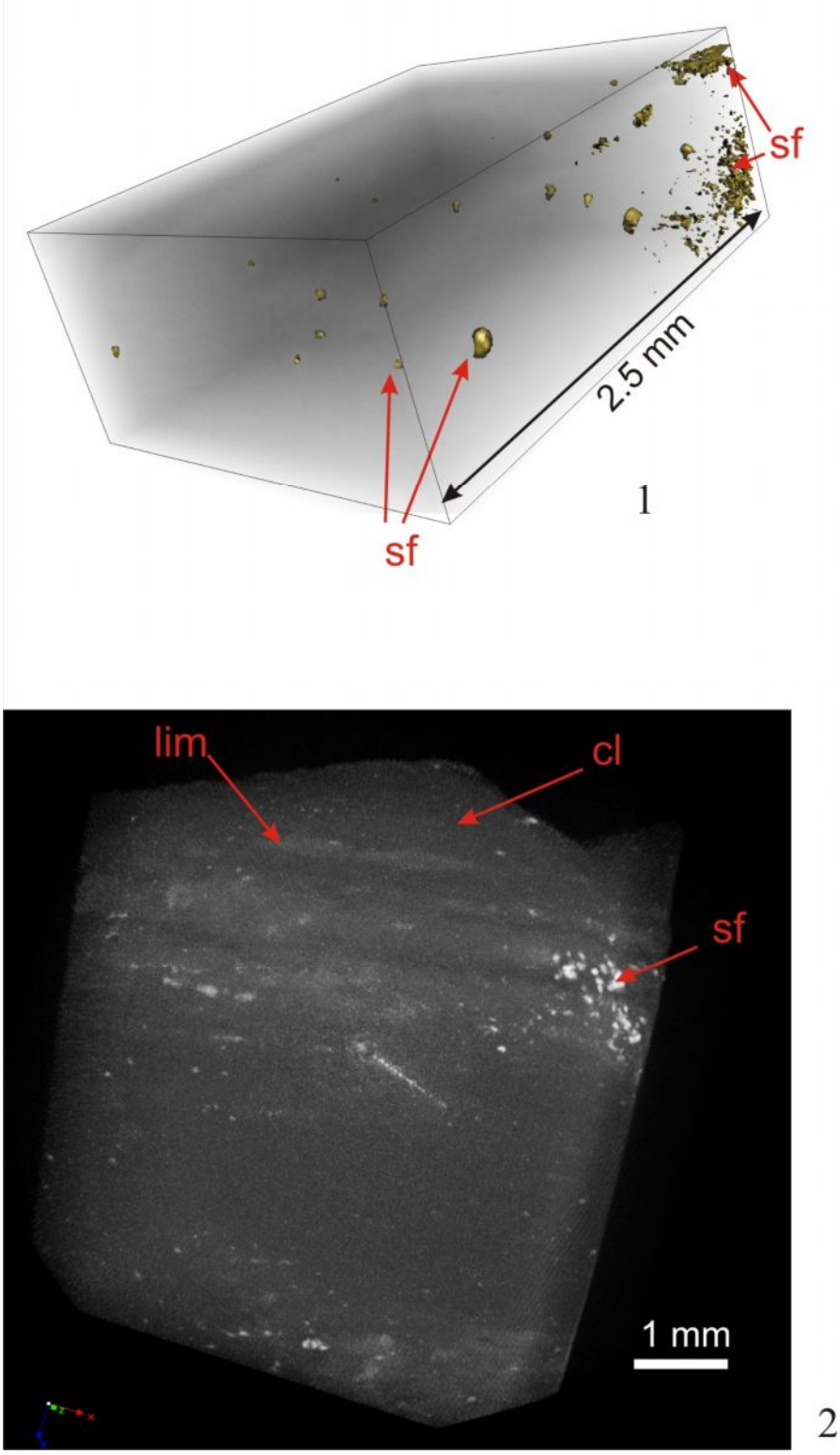

Figure 5. Lithological features observed in X-ray tomograms

1 – Spatial distribution of the sulfide grains (sf) in the clayey limestone, sample HM-1-18; Timan-Pechora Basin, western part of the Kosyu Depression, borehole 1-Kharutamylk, depth 3367 m, Upper Devonian, Frasnian. Visualization with Voxler software.

2 – Microstructure of the domanicoid: cl – mud matrix; lim – carbonate layers; sf – sulfides; sample HM-1-14; Timan-Pechora Basin, western part of the Kosyu Depression, borehole 1-Kharutamylk, depth 3402 m, Upper Devonian, Frasnian. Visualization with CTVox software.

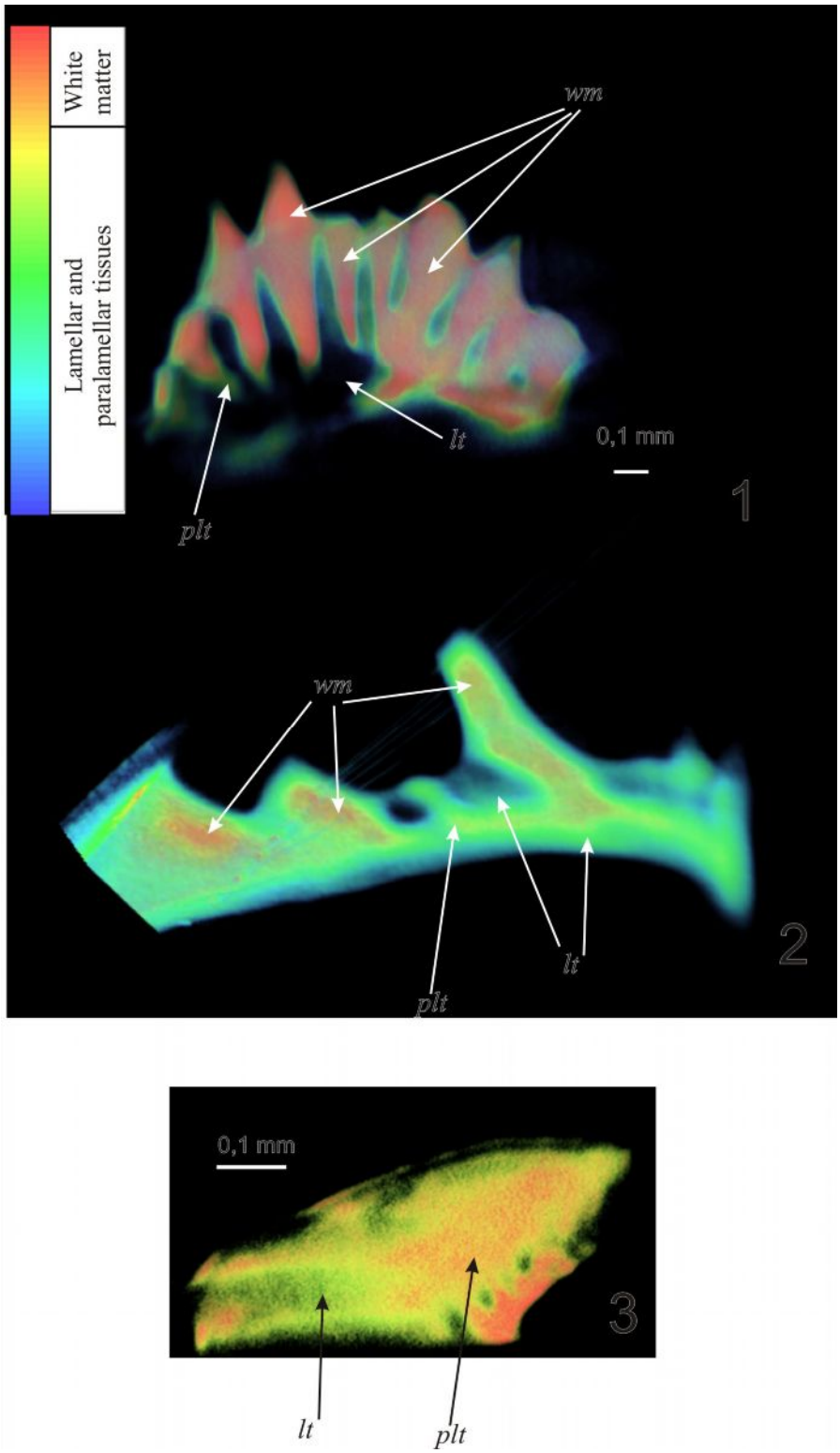

Figure 6. 3D histological models of conodont elements based on the optic tomograms
(visualization with VolView 3 software)

1. - Mehlina fitzroyi (Druce), Pa element, sample 5102a-1; Main Devonian Field, Ilmen Lake; Upper Devonian, Frasnian, Polygnathus ilmenensis local conodont zone.
2. – Sc element of Polygnathidae, sample 5102a-1; Main Devonian Field, Ilmen Lake; Upper Devonian, Frasnian, Polygnathus ilmenensis local conodont zone.
3. - Siphonodella quadruplicata (Branson et Mehl), Pa element, sample 0-7K; Polar Urals, Konstantinov Creek; Lower Carboniferous, Tournaisian, Siphonodella quadruplicata Zone .
plt – paralamellar tissue; lt – lamellar tissue; wm – white matter.

The optic tomograms demonstrate prominent differentiation of the hard tissues of the conodont elements in spite of high "noise" level. However only thin conodont elements, which are translucent in the visible light, are suitable for study with the optic tomography.

Volumes composed by the "white matter", lamellar and paralamellar tissues are distinguishable in the optic tomograms (Figure 6). Attenuation coefficients of the conodont element matter vary from 0.02 (lamellar tissue) to 0.25 mm^{-1} ("white matter").

Optic tomograms permit to improve histological models of conodont elements, which are used for conodont diagnostics in thin sections [Zhuravlev, 2002].

Lithological objects

High attenuation coefficients of the sedimentary rocks restrict applications of the optic tomography in lithological researches. It is possible studying thin translucent rock slabs only. Thin silicite slab (0.4 mm thick) was used as a test object. Resulted optic tomogram characterized by high noise level demonstrates general lumpy structure of the studied sample (Figure 7).

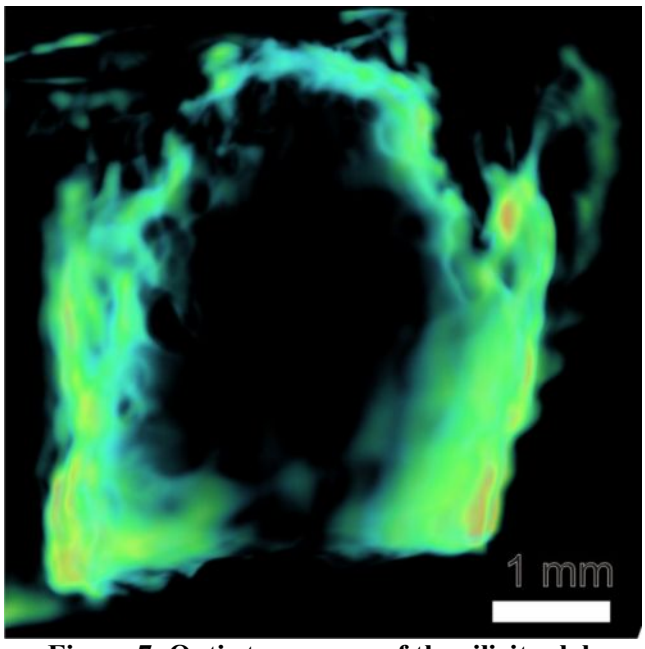

Figure 7. Optic tomogram of the silicite slab
(sample Tn-16-1/99; Polar Urals, Konstantinov Creek; Lower Carboniferous, Tournaisian)
Visualization with VolView 3 software.

Conclusions

Study of the possible CT applications in micropalaeontology and lithology suggests the following conclusions:

1. X-ray micro-CT is applicable for conodont diagnostics in the host rocks (avoiding special sample preparation), granulometric study of the detritic carbonates, porosity evaluation, and

determination of the sulfide concentration. Samples came from the reference collections can be studied with this nondestructive method.

2. The optic microtomography promises results in histological study of conodont elements. Additionally this method can be used for nondestructive study of the structure of the translucent rock slabs (e.g. silicites).

3. Tomogram-based 3D models of the studied objects are suitable for both the micropalaeontological and lithological investigations.

References

Zhuravlev A.V. *Gistologiya i mikroskul'ptura pozdnepaleozoyskikh konodontovykh elementov* [Late Palaeozoic conodont element histology and micro-ornamentation]. Saint Petersburg.: Geoservis Plyus, 2002, 94 p.

Arns C.H., Bauget F., Limaye A., Sakellariou A., Senden T.J., Sheppard A.P., Sok R.M., Pinczewski W.V., Bakke S., Berge L.I., Oren P.-E., and Knackstedt M.A. Pore-Scale Characterization of Carbonates Using X-Ray Microtomography. Society of Petroleum Engineers Journal. Volume 10, Number 4. 2005. P. 475-484.

Błażejowski, B., Binkowski, M., Bitner, M. A., and Gieszcz, P. X−ray microtomography (XMT) of fossil brachiopod shell interiors for taxonomy. Acta Palaeontologica Polonica. 56(2). 2011. P. 439-440.

Frank-Kamenetskaya O.V., Rosseeva E.V., Zhuravlev A.V., Rozhdestvenskaya I.V., Banova I.I., Simon P., Buder J. Carrillo-Cabrera W., Kniep R. Hard tissues of S-elements of late Paleozoic conodont: microstructural and crystallographic aspects. Fedorov Session 2008. Abstracts. RMS DPI 2008-2-72-1. 2008. P.229-231.

Goudemanda N., Orchard M. J., Urdy S., Bucher H., and Tafforeau P. (2011). Synchrotron-aided reconstruction of the conodont feeding apparatus and implications for the mouth of the first vertebrates // PNAS Early Edition. www.pnas.org/cgi/doi/10.1073/pnas.1101754108

Johns, R. A., Steude, J.D., Castanier, L.M., Roberts, P.V. Non destructive measurements of fracture aperture in crystalline rock cores using X-ray computed tomography. J. Geophys. Res. 98, 1993. P. 1889–1900.

Ketcham, R.A., and Carlson, W.D. Acquisition, optimization and interpretation of X-ray computed tomographic imagery: Applications to the geosciences. Computers & Geosciences, v. 27, 2001. P. 381–400.

Peters, E.J., Afzal, N. Characterization of heterogeneities in permeable media with computed tomography imaging. J. Pet. Sci. Eng. 7.1992. P. 283–296.

Tafforeau P., Boistel R., Boller E., Bravin A., Brunet M., Chaimanee Y., Cloetens P., Feist M., Hoszowska J., Jaeger J.-J., Kay R.F., Lazzari V., Marivaux L., Nel A., Nemoz C., Thibault X., Vignaud P., Zabler S. Applications of X-ray synchrotron microtomography for non-destructive 3D studies of paleontological specimens. Applied Physics A**.** 83. 2006. P. 195–202.

Wellington, S.L., Vinegar, H.J. X-ray computerized tomography. Journal of Petroleum Technology 39, 1987. P. 885–898.

Withjack, E.M. Computed tomography for rock property determination and fluid flow visualization. SPE Formation Evaluation, vol. 3, no. 4. 1988. P. 696-704.

Zalewska J., Kaczmarczyk J. Analysis of rock samples' internal pore structure based on X-ray computed microtomography data. Part I. NAFTA-GAZ. LXVII. 2011. P. 533-544.